J Electroceram (2008) 20:35–41
DOI 10.1007/s10832-007-9333-x

Influence of electric field on the ultrasound velocity in PZT ceramics

V. Ryzhenko · L. Burianova · P. Hana

Received: 23 February 2007 / Accepted: 12 September 2007 / Published online: 20 October 2007

Abstract The paper deals with the influence of the electric bias field on the ultrasound velocity of various samples of Pb $(Zr_xTi_{1-x})O_3$ (PZT) ceramics. The ultrasonic velocities were measured on commercial types of PZT ceramics as APC 841, APC 850, and APC 856, at room temperature. The comparison of the ultrasound velocities dependence on electric bias field was made for poled/unpoled soft ceramics. The ultrasonic pulse-echo technique was used in our experiment. The ultrasonic system is based on Matec Instruments, Inc. modules. The time domain response was recorded and time of flight between echoes was directly measured by digital oscilloscope, type Agilent 54622D. The high bias field was applied on disk samples by the high voltage amplifier type Trek 610D, using a special setup and sample holder. The sound velocity was found to change drastically near the coercive field for a PZT ceramics, where the velocity of longitudinal waves decreases with an increasing field while the velocity of shear waves increases, which is caused by the change of the elastic anisotropy under influence of the depolarization field. The consequent change of the piezoelectric contribution to effective elastic constant decreases the velocity of longitudinal waves and at the same time increases the velocity of shear waves around the coercive field.

Keywords PZT ceramics · Longitudinal and shear waves · Ultrasonic phase velocity and attenuation

V. Ryzhenko (✉) · L. Burianova · P. Hana
Department of Physics and International Center for Piezoelectric Research, Technical University of Liberec,
Halkova 6,
CZ-461 17 Liberec 1, Czech Republic
e-mail: volodymyr.ryzhenko@tul.cz

1 Introduction

Lead zirconate titanate (PZT) ceramics is the most important commercial piezoelectric material because of its adjustable properties, and the ability of tailoring its properties, either by changing the composition or by acceptor or donor doping.

The pulse-echo techniques are widely used for ultrasonic velocity measurements and elastic constant determination for various materials, such as PZT ceramics [1, 2], PZN-PT single crystals [7, 8], diamond, lanthanum aluminosilicate glasses, lanthanum gallogermanate glasses, triglycine sulfate single crystals, and other materials. In [2] the ultrasonic velocities and dielectric constants were measured along different directions in X–Z plane of PZT ceramics (poling direction is along Z-axis). A complete set of the values of elastic stiffness constants and piezoelectric $e_{i\lambda}$ – and $d_{i\lambda}$ – constants has been obtained by the least squares method from the wave velocities and dielectric constants. Ceramic samples were poled by DC field, when the samples were cooled down from temperatures above the Curie temperature. The ultrasonic velocities were measured at room temperature by an ultrasonic–pulse-echo overlap method using a Matec Pulse Modulator&Receiver Model 6600, a Decade Dividers & Dual Delay Generator Model 122B and a 5 MHz 0.5 transducer (Harisonic Labs., Inc). In [3], the dispersion of ultrasound velocity and attenuation of piezoceramics PZT were investigated using ultrasonic sprectroscopy in the frequency range of 20–60 MHz. In the investigated frequency range, velocity dispersion of 1–3 m/s per MHz was observed. The attenuation depends nonlinearly on frequency. The shear waves exhibited an order of magnitude larger attenuation than the longitudinal ones. Domain switching behavior of PZN-PT ferroelectric single crystal has been investigated using the ultrasonic technique

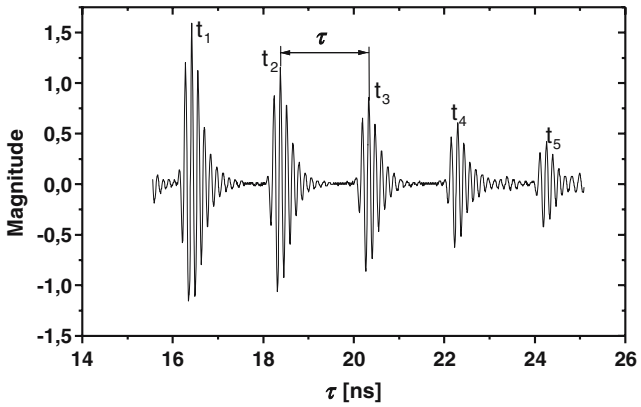

Fig. 1 The response of shear ultrasonic wave in PZT ceramics

in addition to the polarization hysteresis measurements. The sound velocity changes drastically near the coercive field for this material, which reflects that domain polarization rotation, occurred during polarization switching. A complete set of velocity versus electric field loops was measured quasi-statically in a switching cycle and they were compared with the polarization hysteresis loop [8, 9]. In [4], the velocity of ultrasound in a group of lanthanum gallogermanate glasses was obtained by the ultrasonic pulse-echo measurements, at room temperature. Both longitudinal and transverse wave velocities of these glasses depend on the composition. The experimental results were used to obtain the elastic constants. The longitudinal ultrasonic attenuation and velocity were measured in triglycine sulfate (TGS) single crystal over the temperature range 30–100°C [5]. The temperature dependence of elastic properties of a series of lanthanum gallogermanate glasses were determined by ultrasonic pulse-echo techniques. The measurements were performed on the Panametric model 5800 pulser/receiver, and with two especially designed high temperature PZT transducers from Etalon Inc., in temperature up to 350°C and at 20 frequency [6].

2 Theoretical backgrounds

The propagation of a plane wave in solids is governed by Christoffel equation.

Defining the quantities:

$$\Gamma_{il} = c^{E}_{ijkl} n_j n_k,\ \gamma_i = e_{kij} n_j n_k,\ \varepsilon = \varepsilon^{S}_{jk} n_j n_k,$$

we can write this equation for piezoelectric solids in this way:

$$\rho \cdot V^2 \cdot n_i = \left(\Gamma_{ij} + \frac{\gamma_i \gamma_j}{\varepsilon}\right) \cdot n_j \tag{1}$$

where c^{E}_{ijkl}, e_{kij} and ε^{S}_{ijk} are the elastic stiffness constants, measured under constant electric field, piezoelectric stress coefficients and dielectric constants measured under constant strain, respectively, n_i is component of the unit vector $\vec{n}$ of the wave propagation direction and Γ_{ij} is the Christoffel's tensor, ρ is the density, V is the ultrasound velocity [10].

3 Experiment

3.1 Measurement of the phase velocity and the attenuation

The phase velocity V of the wave can be generally expressed as a ratio of the thickness d of the sample and time of flight τ of the ultrasonic echoes, which are generated by reflections at a pair of parallel surfaces of the sample. The linear function of times of flights on order of response i is used to get the averaged velocity $\overline{V}$ from response spectrum in Fig. 1:

$$t_i = t_1 + \tau \cdot i, \quad i = 1,\ 2 \ldots n \quad \overline{V} = \frac{2d}{\tau} \tag{2}$$

Figure 1 shows a train of echoes from multiple round-trips through the PZT sample. The time τ between two successive echoes is the time required for the pulse to travel through the sample and back to the transducer.

The relative attenuation coefficient α can be generally expressed in standard units as

$$\alpha = -\ln\frac{A_{n+1}}{A_n}\Big/2d \quad \left[\text{neper} \cdot m^{-1}\right] \quad \text{or in other units} \quad -10\log\frac{A_{n+1}}{A_n}\Big/2d \quad \left[dB \cdot m^{-1}\right] \tag{3}$$

where $2d$ is the travel distance of the wave, i.e. for one transducer method it is thickness of the sample multiplied by two, and A_i is the magnitude of ith echo response.

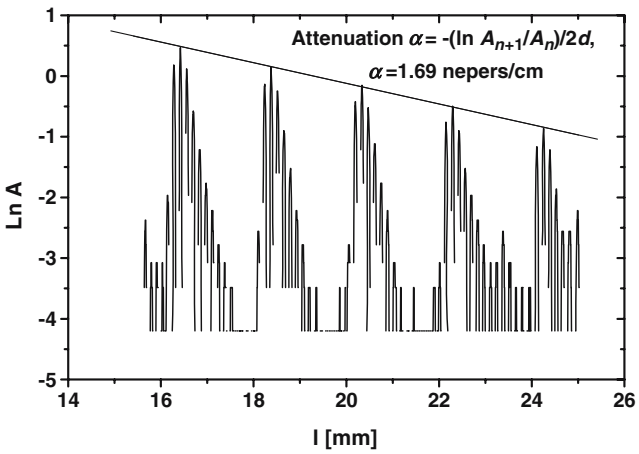

Fig. 2 The logarithmic response of PZT ceramics. The slope of the *solid line* is proportional to α

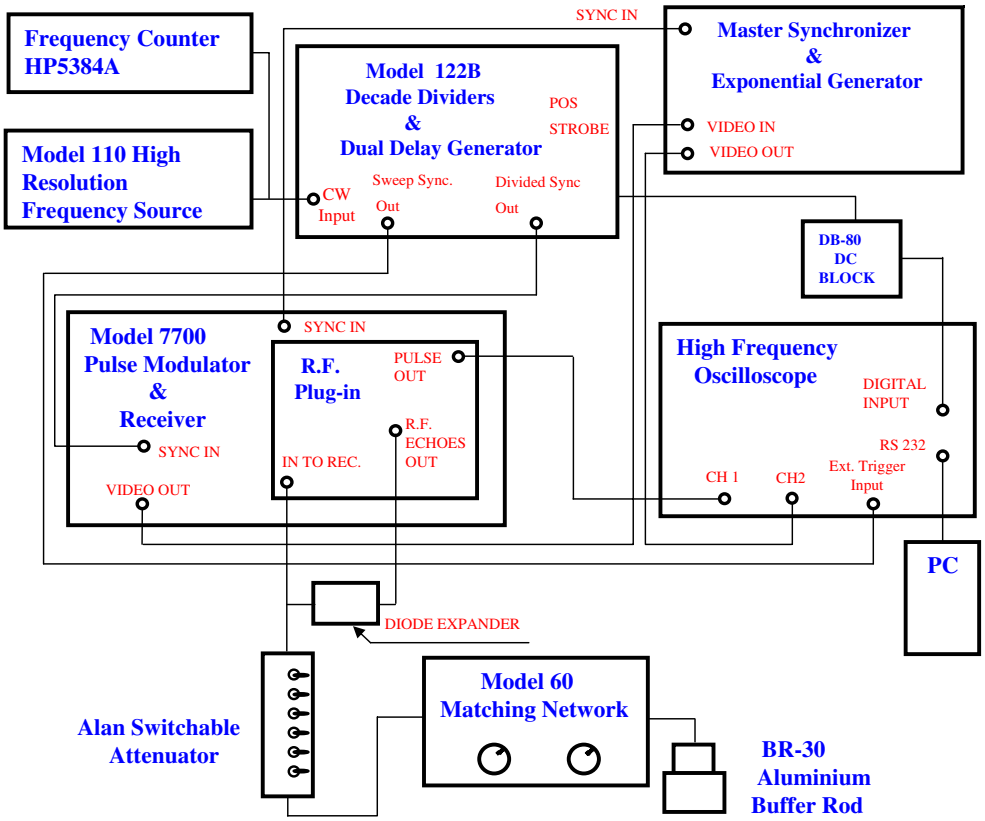

Fig. 3 Experimental setup

The value of relative attenuation α equals tangent of a linear function (3) $\ln\frac{A_{n+1}}{A_n}$ vs. travel distance $2d$, see Fig. 2.

3.2 Poled ceramic samples

The poled PZT type ceramics exhibit averaged crystal symmetry ∞mm. Typically the poling direction of ceramic samples is [001] direction.

The relations between the linear elastic coefficient c_{44}^E and the velocity of shear waves propagating along the [001] direction can be expressed as:

$$c_{44}^E = \rho\left(v_{\text{shear}(010),(100)}^{(001)}\right)^2 \tag{4}$$

The relations between the velocity of longitudinal waves propagating along the [100] direction and the linear elastic coefficient c_{11}^E was expressed as:

$$c_{11}^E = \rho\left(v_{\text{long}}^{(100)}\right)^2 \tag{5}$$

Electrically clamped conditions are supposed for the high fundamental frequencies of used transducers, which are operating at 15 and 22 MHz.

3.3 Experimental setup

The ultrasonic pulse-echo technique was used in our experiment. The ultrasonic system is based on Matec Instruments, Inc. modules. The time domain response was recorded and time of flight between echoes was directly measured by digital oscilloscope, type Agilent 54622D. The high bias field was applied on disk samples by the high voltage amplifier type Trek 610D, using a special setup and sample holder.

The ultrasound velocities were measured using the experimental setup as shown in Fig. 3. Various transducers for generation of ultrasound waves were used: a commercial Lithium Niobate transducers (Valpey Fisher, type DP152-0.25″ with polystyrene delay and SD152-FL with fused silica delay) with fundamental frequency 15 MHz for longitudinal and shear waves and a shear wave transducer 7×14 mm^2, $LiNbO_3$, with metallic coupling layer to glass delay line working at 22 MHz. The Pulse Modulator & Receiver Model 7700 generated the tone burst pulses and the Plug-in Model 755, 0.5–22 MHz, received R.F. echoes. The ultrasonic system was based on Matec Instruments, Inc. modules. The electric DC bias field was applied by HV amplifier Trek model 610D. The time domain response was recorded and time of flight between echoes directly measured by digital oscilloscope, type Agilent 54622D. A

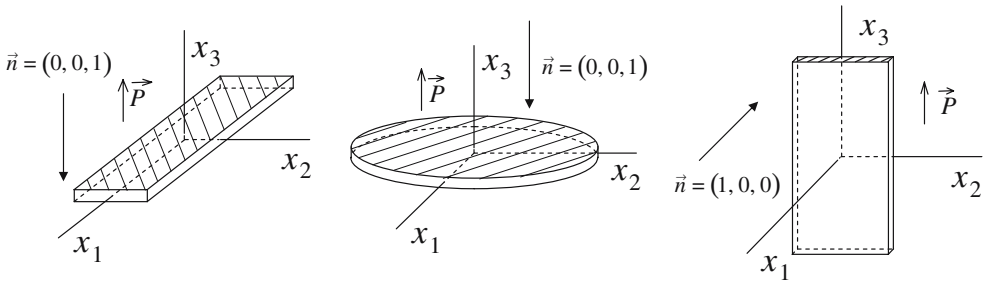

Fig. 4 Measured samples placed in coordinate axes system

pulse echo-overlap technique was used for the determination of the absolute values of velocity, with which the high precision – better than 1% can be obtained.

PZT ceramic samples of type APC856 (soft), APC850 (soft) and APC841 (hard) were provided by American Piezoceramics International, Mackeyville, PA, USA. Disk shaped samples of type APC841, APC850 were 10 mm in diameter, 1 mm in thickness. The samples were polarized in direction of their thickness and measured in the same [001] direction.

Rectangular plate samples of type APC841, APC850, APC856 with dimension 7×14×1 mm were polarized along their thickness or length directions. Samples were measured in [100] direction and/or in [001] direction. Both unpoled and samples polarized by manufacturer were measured. Figure 4 shows types of measured samples placed in coordinate axes system. Electrode pattern, directions of polarization and wave propagation are shown.

4 Results and discussion

The measurement of PZT samples under DC bias electric field was realized inside the special sample holder, see Fig. 5. The samples were protected in oil bath from sparking on edges of samples. Thin aluminum foil was used as removable electrodes. The good electric conductivity and ultrasonic coupling were realized by suitable coupling material. A honey was used as a very good material for shear wave coupling at frequencies 10–20 MHz at room temperature. We can observe the poling process on virgin sample in electric field, on Figs. 6 and 7. Figures 8, 9 and 10 show hysteresis loops of ultrasonic velocity versus bias electric field. The measurements were realized in a special sample holder connected to Matec ultrasound system controlled by computer. The PZT ceramic samples used were poled by manufacturer.

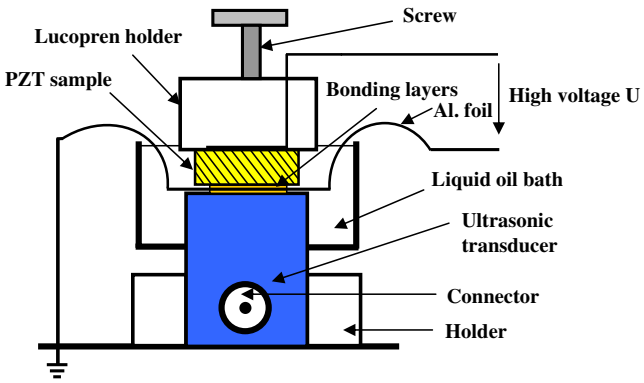

Fig. 5 A sample-holder for measurements of PZT ceramic samples under high voltage DC bias

At the beginning of the measurements, the electric field was applied in the direction opposing the sample polarization. When the field was gradually increased, the longitudinal velocity was almost unchanged until the electric field magnitude reaches approximately 13 kV/cm for both positive and negative field directions. The velocity begins to decrease quickly with increasing field when above the critical points. The velocity reaches a minimum in the vicinity of the coercive field E_c and then drastically increases back to its original value, if the field level increases (Figs. 8 and 9).

For shear waves, the velocities start to increase with increasing electric field and reach maxima near the coercive field E_c. Above these critical points, the velocity falls down with increasing electric field and reaches a minimum. With electric field decreasing, the velocity increases to the original value (Fig. 10). Asymmetrical hysteresis loops for

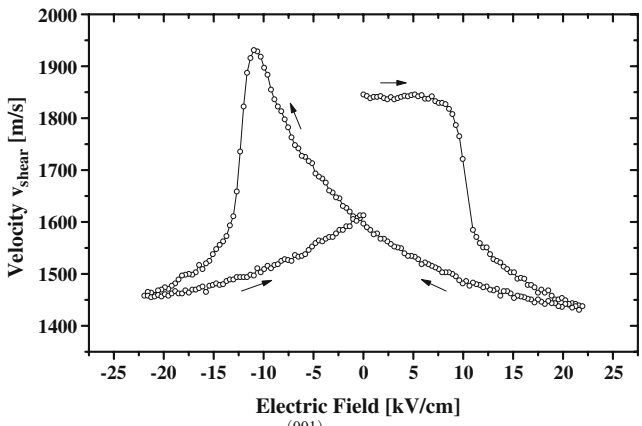

Fig. 6 Shear mode velocity $v^{(001)}_{\text{shear}\,(100),(010)}$ as a function of electric field on unpoled sample of PZT ceramic APC 850, disk 10 mm in diameter, 1 mm in thickness

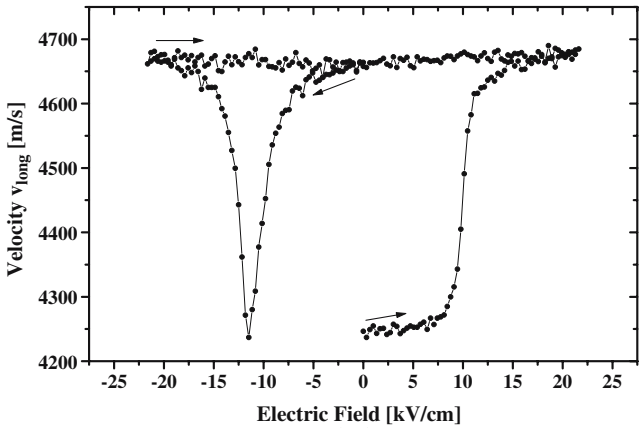

Fig. 7 Longitudinal mode velocity $v_{\text{long}}^{(001)}$ as a function of electric field on unpoled sample of PZT ceramic APC 850, disk 10 mm in diameter, 1 mm in thickness

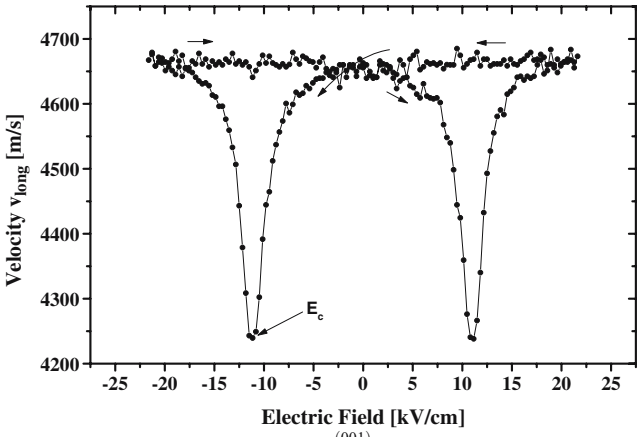

Fig. 9 Longitudinal mode velocity $v_{\text{long}}^{(001)}$ as a function of electric field for the sample of PZT ceramic APC 850, disk 10 mm in diameter, 1 mm in thickness. Sample was not polarized

hard ceramics were observed, which is due to the domain pinning effect by the oxygen vacancies in hard materials.

The change of acoustic attenuation during polarization for shear mode ultrasound wave is shown in the Fig. 11.

In Table 1 we collected velocity measurements and some elastic constants, calculated from the measurements of the velocities of longitudinal and shear waves in absence of applied electric field for poled samples at room temperature. The results show that the elastic modulus c_{11}^E of the hard ceramics APC 841 is approximately 15% higher then the elastic modulus of the soft ceramics (APC 850, APC 856).

PZT ceramics are in ferroelectric phase with various possible domain states at room temperature. The dipole of each unit cell could be formed along the allowed directions. During application of the electric field, some orientations of polarization become energetically preferable. Direction of polarization follows external electric field.

From Eq. 4 the relation between the velocity of shear waves propagating along the [001] direction and the linear elastic coefficient c_{44}^E for [001] poled sample is:

$$v_{\text{shear}(010),(100)}^{(001)} = \sqrt{\frac{c_{44}^E}{\rho}} \tag{6}$$

During repolarization process by applying reverse electric field, the polarization directions jump to energetically preferable states, which lead to the increment of perpendicular component of polarization and piezoelectric contribution to the propagation of transversal mode of ultrasonic waves (see Eqs. 7 and 8):

$$v_{\text{shear}(001)}^{(100)} = \sqrt{\frac{d_{15}^2 \cdot \left(c_{44}^E\right)^2 + c_{44}^E \cdot \varepsilon_{11}^S}{\rho \cdot \varepsilon_{11}^S}} \tag{7}$$

$$v_{\text{shear}(010)}^{(100)} = \sqrt{\frac{c_{11}^{\text{E}} - c_{12}^{\text{E}}}{2\rho}} \tag{8}$$

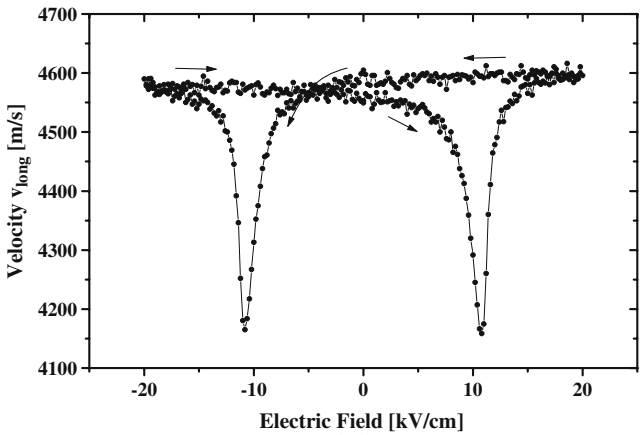

Fig. 8 Longitudinal mode velocity $v_{\text{long}}^{(001)}$ as a function of electric field on poled sample of PZT ceramic APC 850, disk 10 mm in diameter, 1 mm in thickness

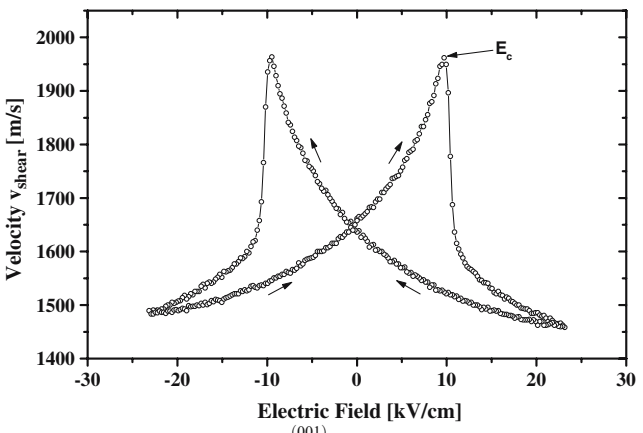

Fig. 10 Shear mode velocity $v_{\text{shear}\,(100),(010)}^{(001)}$ as a function of electric field for poled sample of PZT ceramic APC 850, disk 10 mm in diameter, 1 mm in thickness

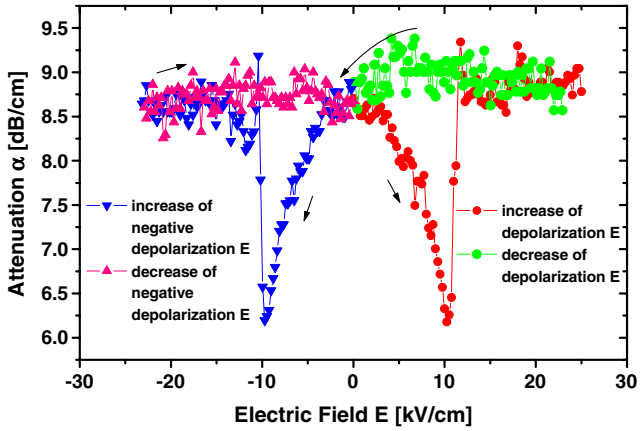

Fig. 11 Attenuation of shear wave as a function of electric field on poled sample of PZT ceramic APC 850, disk 10 mm in diameter, 1 mm in thickness

where $c^E_{\lambda\mu}$ and $d_{i\lambda}$ denote the elastic stiffness constants under constant electric field and piezoelectric charge constants in matrix notation, respectively.

The situation is found to be opposite for the case of longitudinal waves. The relationship between the velocity of longitudinal waves propagating along the [001] direction (including contribution of the piezoelectric effect) and the linear elastic coefficients c^E_{33} and c^E_{13} for [001] poled sample is:

$$v^{(001)}_{\text{long}} = \sqrt{\frac{\left(c^E_{13}\cdot 2d_{31} + d_{33}\cdot c^E_{33}\right)^2 + c^E_{33}\cdot \varepsilon^S_{33}}{\varepsilon^S_{33}\cdot \rho}} \tag{9}$$

With increasing perpendicular component of polarization, the piezoelectric contribution to the propagation of longitudinal mode of ultrasonic waves is found to decrease (see Eq. 10).

$$v^{(100)}_{\text{long}} = \sqrt{\frac{c^E_{11}}{\rho}} \tag{10}$$

Different shapes of hysteretic loops for longitudinal and shear mode waves propagation are probably caused by distribution of local polarization. In case of hysteretic loop for longitudinal wave propagation, the stabilization effect of external electric field on local polarization is present. The shear wave hysteretic loop response exhibits butterfly shape due to the random distribution of polarization direction in plane perpendicular to applied electric field.

5 Conclusion

Ultrasonic velocities and attenuation measurements of PZT ceramics have been carried out with the ultrasonic measurements under DC bias electric field. Velocities were measured using a pulse-echo technique at room temperature. The velocity, measured on poled samples was found to be higher than that ones in longitudinal mode, while the shear mode waves behaved by reversal way.

The strong influence of phase velocity and ultrasound attenuation on electric fields was observed. The change of phase velocity for unpoled and poled states of PZT is above 9% for longitudinal and 16% for shear mode velocity, respectively.

The velocity of longitudinal waves decreases with an increasing field while the velocity of shear waves increases, which is caused by the change of the elastic anisotropy under influence of the depolarization field. The consequent change of the piezoelectric contribution to effective elastic constant decreases the velocity of longitudinal waves, meanwhile increasing the velocity of shear waves around the coercive field.

The study of the influence of poling and/or bias electric field on propagation of the ultrasound in a PZT ceramics shows new possibilities of tuning mechanical properties of ceramics by electric field. The study of the ultrasound propagation in PZT ceramics also enables the determination of a set of elastic and piezoelectric constants, and the investigation of domain polarization reorientation and estimation of the presence of structural phase transitions.

Table 1 Measured velocities of longitudinal and shear waves and some calculated elastic constants.

Sample	Velocity [m/s]					Elastic moduli [10^9, Pa]	
	$v^{(100)}_{\text{long}}$	$v^{(001)}_{\text{long}}$	$v^{(100)}_{\text{shear}(001)}$	$v^{(100)}_{\text{shear}(010)}$	$v^{(001)}_{\text{shear}(010),(100)}$	c^E_{11}	c^E_{44}
APC 841	4,423		2,542	2,148		148.7±1.4	
APC 841		4,690			1,857		26.2±0.3
APC 850		4,565			1,651		21.0±0.1
APC 850	4,145		2,302	1,797		132.3±0.8	
APC 856	4,130		2,247	1,870		127.9±0.4	

Acknowledgment This work was supported by the Grant Agency of the Czech Republic (GACR 202/07/1289).

References

1. H. Wang, W. Cao, J. Appl. Phys. **92**, 4578 (2002)
2. Y. Sasaki, T. Ochiai, Y. Takeuchi, S. Hayashi, Jpn. J. Appl. Phys. **34**, 4122 (1995)
3. H. Wang, W. Jiang, J. Appl. Phys. **85**, 8083 (1999)
4. L.G. Hwa, W.C. Chao, Mat. Chem. Phys. **94**, 37 (2005)
5. J.R. Su, C.F. Zhu, M. Wang, Z.G. Zhu, Mater. Res. Bull. **34**(12–13), 1885 (1999)
6. L.G. Hwa, W.C. Chao, S.P. Szu, Mater. Res. Bull. **37**(7), 1293 (2002)
7. P. Hana, L. Burianova, E. Furman, S. Zhang, T.R. Shrout, V. Ryzhenko, P. Burry, Ferroelectrics **319**, 371 (2005)
8. J. Yin, W. Cao, Appl. Phys. Lett. **80**, 1043 (2002)
9. J. Yin, W. Cao, Appl. Phys. Lett. **79**, 4556 (2001)
10. D. Royer, E. Dieulesaint, *Elastic Waves in Solids I* (Springer, Berlin, Heidelberg, New York, 2000), p. 178